Advanced Physical Research
Vol.4, No.1, 2022, pp.22-32

INFLUENCE OF Ag-DOPING-COBALT OXIDE ON THE STRUCTURE, OPTICAL PROPERTIES, MORPHOLOGY AND PREFERENTIAL OXIDATION ACTIVITY OF CO

S. Barkaoui[1], S. Chakhari[2], S. Kouass[3], H. Dhaouadi[1], G. Imanova[4*], F. Touati[1]

[1]Laboratoire Matériaux Traitement et Analyse INRAP, Technopôle Sidi-Thabet, Tunis
[2]Laboratory of Materials Chemistry and Catalysis, Chemistry Department, Faculty of Sciences of Tunis, University of Tunis El Manar, Tunis
[3]Laboratoire des Matériaux Utiles, INRAP, Technopôle Sidi-Thabet, Tunis
[4]Institute of Radiation Problems, ANAS, Baku, Azerbaijan

Abstract. Undoped and doped mesoporous silver/Co_3O_4 nanorods supported on stainless steel wire meshes were prepared using the ammonia-evaporation-induced method. In the paper the crystalline nature and phase purity of the as-prepared materials were investigated using X-ray diffraction (XRD) measurements. Morphological characterizations were performed using a scanning electron microscope (SEM). The band gap energies were estimated by UV-vis spectroscopy. The results for optical properties results showed an apparent decrease in the direct band gap energies with increasing Ag-content from 1.86 eV for pure Co_3O_4, to 1.58 eV for 24%Ag/Co_3O_4. The preferential oxidation CO reaction results showed that the undoped Co_3O_4 exhibits a good catalytic activity in the [170-195°C] temperature range, while the catalytic activity is weakly affected by the Ag-doping process. The enhanced optical properties lead to the possible use of said nanorods in photocatalytic and photovoltaic applications.

Keywords: *ammonia-evaporation-induced method, Nanorods, electron microscopy, optical properties, preferential oxidation activity of C.*

Corresponding Author: *G. Imanova, Institute of Radiation Problems, Azerbaijan National Academy of Sciences, AZ 1143, Baku, Azerbaijan, e-mail: gunel_imanova55@mail.ru*

Received: *28 February 2022;* ***Accepted:*** *14 March 2022;* ***Published:*** *20 April 2022.*

1. Introduction

Interestingly, the physico-chemical properties of materials change significantly when the particle size is reduced from bulk to nanomaterial. Large surface-to-volume ratio, shape and particle size provide opportunities for tuning the properties of the material. Cobalt oxide is a technologically important transition metal oxide due to its potential applications in heterogeneous catalysis (Pudukudy & Yaakob, 2014), magnetic materials (Moro *et al.*, 2013) and CO sensors (Gupta *et al*., 2011), in anode materials for rechargeable Li ion batteries (Rahman *et al*., 2009) and solar selective absorber (Avila *et al.*, 2004). Several researchers have studied the optical properties of Co_3O_4 nanoparticles (Makhlouf *et al*., 2013; Sarfaz & Hasanain, 2014; Hosny, 2014; Wang *et al*., 2009; Chen *et al*., 2015). The values for the band gaps in the Co_3O_4 bulk materials have been reported to be 1.48 and 2.19 eV (Zou *et al*., 2008). Generally, the observed blue shift in the band gap was explained as originating in the finite size effects of the nanoparticles (Sarfaz & Hasanain, 2014). Surface area and surface defects play an important role in the optical properties of the metal oxides. It has previously been reported that transition metal ions

(Ag, Cu, etc.) were doped in semiconductor metal oxides (ZnO, CuO, Co_3O_4, etc.) in order to narrow down the band gap for optical absorption in the visible region.

In recent years, it has been known that carbon monoxide is a highly toxic gas. CO carbon monoxide gas is one of the major air pollutants and its presence, even in traces, may cause serious environmental and health problems. Carbon monoxide directly takes part in the formation of ground-level ozone and increases the greenhouse effect due to its transformation into CO_2 and the stabilization of CH_4 in the atmosphere. Therefore, the control of CO content has been an important area of research. It is also essential to remove the CO from reformed gases. Among the various methods available for eliminating CO pollution, catalytic oxidation is an effective technology using metal oxides. Among the transition metal oxides that are potential candidates to be used in this process, the Co_3O_4 catalyst has been widely considered as the best option (Hu *et al*., 2010; Zhao *et al*., 2012).

Furthermore, it has been found that introducing silver into the transition metal oxide systems strongly increases the catalyst activity in the CO oxidation (Zhang *et al*., 2010; Afanasev *et al*., 2012; Sandoval *et al*., 2011). The increase in activity has been often ascribed to the oxygen donation from the surface transition metal oxide sites to the silver species (Guldur & Balikci, 2002), the enhanced redox transitions of silver oxides in the reaction conditions (Craciun *et al*., 2003) and the improved dispersion of silver (Imamura *et al*., 1988; Keshayaraja *et al*., 2000).

It is now widely known that the behaviors of nanophase materials strongly depend on the shape and size of the particles, which is thus a key factor to their ultimate performance and applications (Camargo *et al*.,2009). Much effort has been made to develop synthetic techniques for growing Co_3O_4 nanostructures such as hydrothermal method (Barkaoui *et al*., 2015; Barkaoui *et al*., 2015), pulsed laser deposition (Ahmed *et al*., 2002), chemical vapor deposition (Cheng *et al*., 1998), radiolysis (Alrehaily *et al*., 2013) and the sol-gel method (Baydi *et al*., 1994). Among the numerous methods developed for synthesizing cobalt oxide, the ammonia-evaporation-induced method has been regarded as one of the most convenient and practical techniques (Li *et al*.,2008; Feng *et al*., 2014).

In this study, we report on, for the first time to the best of our knowledge, the ammonia-evaporation-induced method synthesis and physicochemical characterization as well as the optical properties of mesoporous Ag/Co_3O_4 nanorods. The preferential oxidation of CO using silver-doped cobalt oxide nanorods is also tested.

2. Experimental

2.1. Synthesis of undoped Co_3O_4 and Ag-doped Co_3O_4

Stainless steel wire meshes-supported Co_3O_4 catalysts were synthesized by the ammonia-evaporation-induced method. During preparation, 22.5 mL of H_2O and 10 mL of 30 wt% ammonia solution were consecutively poured without agitation into a Teflon vessel containing 10 mmol of $Co(NO_3)_2.6H_2O$ and 5 mmol of NH_4NO_3. The mixture was then magnetically stirred for half an hour in air. The magnet was then removed from the vessel and a rectangular piece (5 × 3 cm) of stainless steel wire mesh (Feng *et al*., 2014) µm wire diameter and 45 µm screen opening that had been previously washed in HNO_3 (4 M) at 60 °C for several hours was introduced into the reaction solution. The vessel with the solution and the mesh was covered by the watch glass and was heated in the oven at 90 °C for 18 hours to allow the nanorods to grow. Before calcination, the cobalt was in the form of cobalt hydroxide on the surface of the Stainless steel wire meshes. The

unclaimed material was impregnated with silver by the dropwise addition of an aqueous solution of $AgNO_3$ (0.21 M). The impregnation step was then repeated in order to obtain the desired amount of silver in the catalyst (2%, 6%, 13% and 24% Ag/Co_3O_4). Finally, all the samples were calcined in air at 300°C.

2.2. Characterization techniques

X-ray diffraction data (XRD) was obtained on an X'Pert Pro Pan-alytical diffractometer with CuK radiation ($\lambda = 0.15406$ nm) and a graphite monochromator. The XRD measurements were carried out by applying a step-scanning method (2θ range from 10 to 70°). The texture of the as-prepared samples was examined using a scanning electron microscope (Zeiss, DSM 942 model) attached with an energy dispersive X-ray analysis setup (EDAX). Nitrogen adsorption isotherms were performed at -196°C on an ASAP 2020 volumetric adsorption system. The BET surface area was determined from the isotherm analysis in the relative pressure range of 0.04 to 0.20. The optical parameters of the samples were calculated from the optical absorbance data recorded in the 200 - 1000 nm wavelength range using a UV-visible spectrometer (Schmadzu-3101 PC).

2.3. Catalytic performance measurements

Catalytic activity tests for preferential oxidation of CO were performed in a six-flow parallel micro-reactor system that allows up to six samples to be simultaneously tested by means of an automatically operated multi-position valve. Each catalyst consisted of a 5 cm x1 cm strip that was rolled up to form a 1 cm-high cylindrical piece. One roll of catalyst was then inserted into each of the six stainless-steel reactors (1/4 in. outer diameter).

With the gas flow rate used in the experiments (200 mL/min), this configuration resulted in a high space velocity of ~55,000/h. The bed temperature was controlled by means of a ceramic-protected thermocouple inserted into the reactor. The samples were heated under a He flow at 200°C for 60 min. The reactant stream was then passed through the catalyst and its catalytic activity and selectivity were evaluated at decreasing temperatures from 200 to 175°C. The reactant gas feed contained 25 vol.% H_2, 0.5 vol.% CO and 0.5 vol.% O_2 in He. The conversion of CO was calculated from CO-conversion (%) = [CO]/[CO]in x 100. Where [CO]in is the inlet carbon monoxide and [CO] is the concentration of carbon dioxide as a product. The reactant gas feed contained 25 vol.% H_2, 0.5 vol.% CO and 0.5 vol.% O_2 in He.

The conversion of CO was calculated from CO-conversion (%) = [CO]/[CO]in × 100.

3. Results and discussions

3.1. X-ray diffraction studies

The XRD patterns of the as-prepared samples (2%, 6%, 13% and 24% Ag/Co_3O_4) are shown in Fig.1. The phase identification for low-doping level 2% and 6% Ag/Co_3O_4 by XRD revealed a single phase with cubic symmetry (Fd-3m). All the diffraction peaks could be indexed to the Co_3O_4 spinel structure (JCPDS file no. 00-009-0418). No additional peaks corresponding to impure phases like silver/silver oxide species were observed implying the complete solubility of Ag ions into the Co_3O_4 lattice, or the doped silver with low composition may be well dispersed in the Co_3O_4 matrix. The Ag^+ ions in the Co_3O_4 lattice behave similarly to other monovalent dopant ions like Na^+ and K^+,

which have the ability to occupy both the lattice and interstitial sites (Zamiri *et al*., 2014). As seen in Fig.1(d), when the silver content reaches 13%, the studied sample is characterized by the Co_3O_4 as the major phase, with some characteristic peaks corresponding to silver oxide (Ag_2O) with a cubic system crystalline structure (JCPDS file no. 00-043-00997) showing a weak intensity.

For the sample with silver content equal to 24% (Fig. 1(e)), the presence of the nanocomposite formed by two distinct phases: Co_3O_4 and $AgCoO_2$ was observed. As seen in Fig.1 (e), the marked peaks (◆) match well the characteristic peaks of the $AgCoO_2$ rhombohedral crystalline system pattern (JCPDS file no. 00-025-0761), indicating the existence of an $AgCoO_2$ phase in the composite.

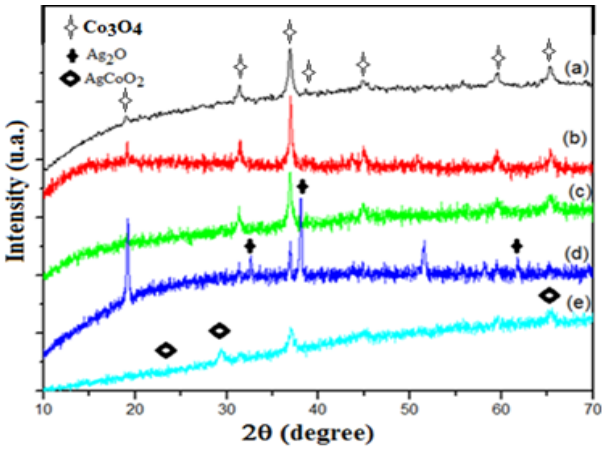

Fig. 1. X-ray powder diffraction pattern of samples calcined at 300°C for 2 h (a): Co_3O_4, (b): 2%Ag/Co_3O_4, (c): 6% Ag/Co_3O_4, (d): 13% Ag/Co_3O_4 and (e): 24% Ag/Co_3O_4

Crystallite sizes (D) of the samples after heating at 300°C were estimated from the broadening of the most intense XRD peak (311) using the Debye-Scherrer approximation (Huang *et al*., 2012).

$$D = 0{,}9\frac{\lambda}{\beta}\cos\theta,$$

where, D is the crystallite size, λ is the X-ray wavelength (0.15406 Å), θ is the Bragg diffraction angle and β is the full width at the half maximum (FWHM) of the diffraction peak.

The crystallite size is found to increase from 31 nm (0%) to 61 nm (13%) with the low Ag-content, as seen in Table 1. This could be explained by the fact that the silver ions Ag^+ could have the ability to occupy both the lattice and interstitial sites. The Ag^+ ion is characterized by the ionic radius of the Ag^+ ion (115 pm), which is larger than that of Co^{3+} (60 pm) /Co^{2+} (70 pm), consequently, the volume of the lattice increases with silver content, affecting the particle size.

When the silver concentration is equal to 24% the particle size decreases to 31nm. At this doping level, the system is characterized by the existence of the $AgCoO_2$ /Co_3O_4 nanocomposite. The minor phase, $AgCoO_2$, could be fixed to the grain boundaries, which prevents the growth of crystal grains and slows down the motion of the grain boundaries (Wang *et al*., 2008). Doping introduced defects could also be a reason for this since the defects prevent grain growth (Ishaque *et al*., 2010; Wu *et al*., 2010).

Table 1. Variation of particle size dependent on the silver content in cobalt oxide (Co_3O_4)

Samples	D (nm)
Co_3O_4	31
2% Ag/Co_3O_4	41
6% Ag/Co_3O_4	43
13% Ag/Co_3O_4	61
24% Ag/Co_3O_4	31

3.2. Morphological study

Fig.2. shows the SEM of the Ag/Co_3O_4 catalyst with different Ag contents. It can be observed that the undoped Co_3O_4 sample is formed by nanorods 30 μm in length and 500 nm wide (Fig.2.). When the Ag-content increases from 2% to 6% (Fig.2.), the morphology doesn't change and remains homogenous.

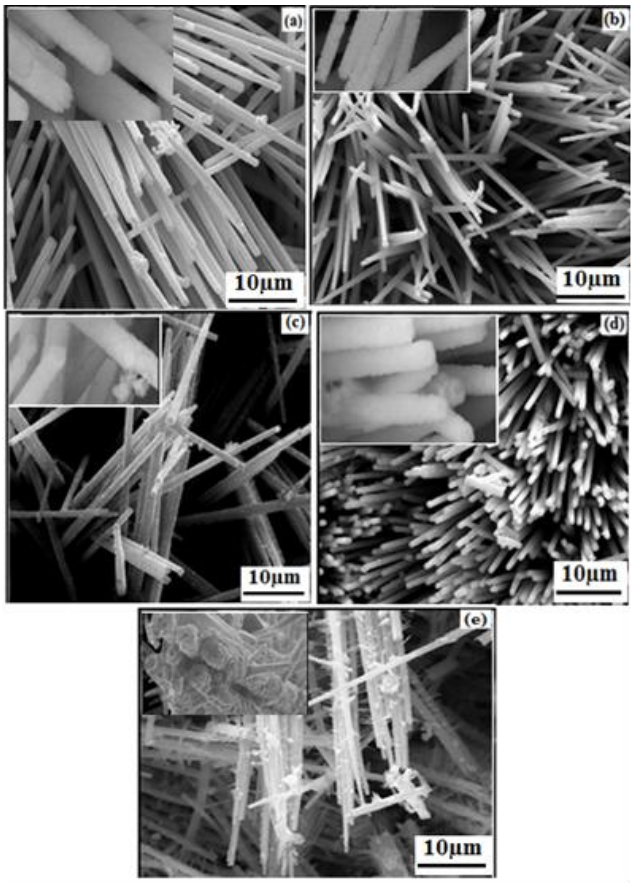

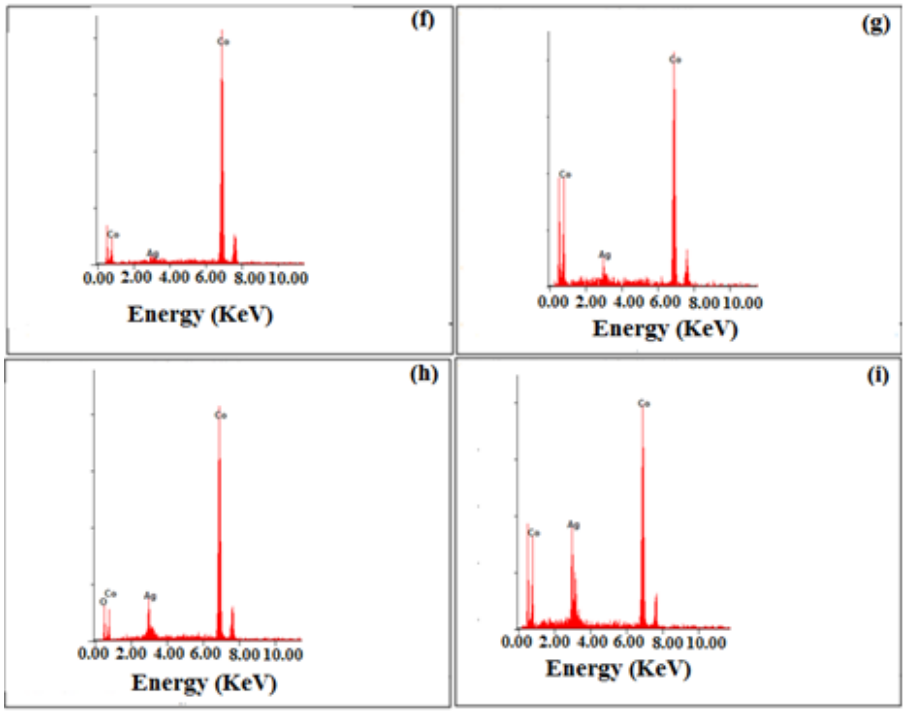

Fig. 2. SEM micrographs of Co_3O_4 nanorods and different Ag contents of Ag/Co_3O_4 nanostructures: (a) pure Co_3O_4, (b): 2%Ag /Co_3O_4, (c): 6% Ag/Co_3O_4, (d):13% Ag/Co_3O_4 and (e): 24% Ag/Co_3O_4 and (f-i) EDX spectra of 2%, 6%, 13% and 24% Ag/Co_3O_4 samples respectively

This indicates that the Ag^+ ions are well dispersed in the cobalt oxide surface. This result is in agreement with those from the XRD, which showed the absence of the characteristic pattern of silver oxide. When the amount of silver becomes equal to or larger than 13%, the nanorods break, which could be due to the formation of silver oxide, Ag_2O, for $13\%Ag/Co_3O_4$ and $AgCoO_2$ for $24\%Ag/Co_3O_4$. An EDX analysis was performed to further confirm the chemical purity of the as-prepared samples. As seen in Fig. 2 (d-f), the lines of Co, Ag and O are clearly observed, in all cases, which confirm that the as-prepared samples were composed of Co, O and Ag elements.

3.3. Optical properties

To investigate the effect of silver doping on the band sates, absorption UV-vis spectroscopy was carried out in order to characterize the optical properties of the as-prepared samples (2%, 6%, 13% and 24% Ag/Co_3O_4) as presented in Fig.3 for the direct allowed band gaps. The incident photon energy (hυ) and the optical band gap energy (Eg) are related to the transformed Kubelka-Munk function $(F(R) \times h\upsilon) = \alpha = A(h\upsilon - Eg)^n$, where the optical absorption coefficient (α) can be calculated using reflectance data according to the Kubelka-Munk equation (Gozuak *et al*., 2009), $F(R) = \alpha = (1 - R)^2/2R$, where R is the reflectance data, A is the constant dependent on transition probability, and n depends on the nature of the transition (n = ½ for allowed direct transition and n = 2 for indirect allowed transition).

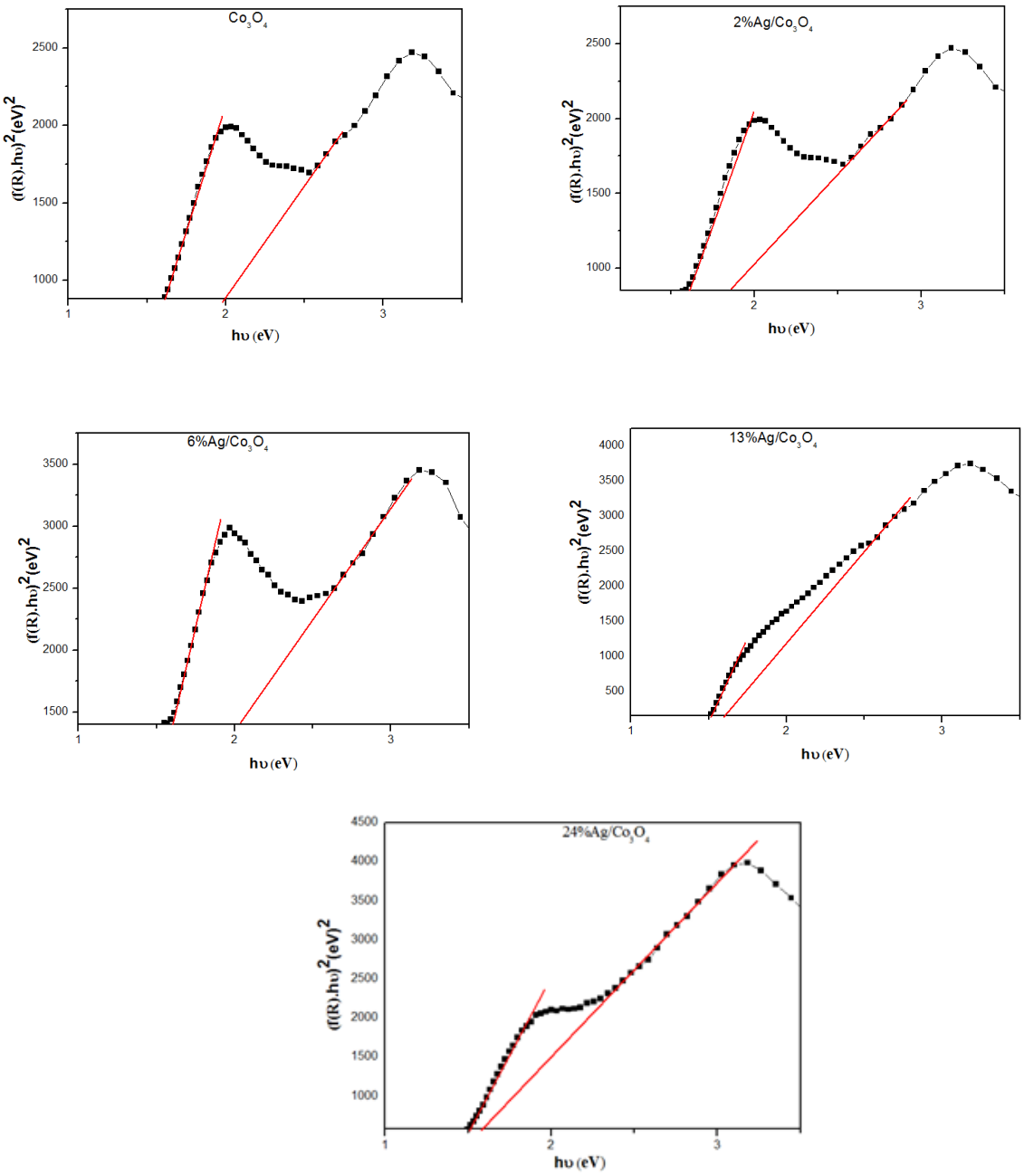

Fig. 3. The Tauc plot ($(F(R).h\nu)^2$ versus hν) to calculate the band energy gap by extrapolating α = 0 of the as-prepared 2%, 6%, 13% and 24% Ag/Co_3O_4 samples

The plots of $(F(R).h\nu)^2$ versus hν, for the 2%, 6%, 13% and 24% Ag/Co_3O_4 samples are shown in Fig.3. The variations of $[F(R).h\nu]^2$ versus hν are straight lines in the higher and lower energies, indicating the presence of direct optical transitions. The values of the band gap energy for 2%, 6%, 13% and 24% Ag/Co_3O_4 were estimated by linear extrapolation of the line to the photon energy axis. Each curve in Fig.3 can be linearly fitted to two lines, which correspond to two band gap energies, Eg_1 and Eg_2 ($Eg_1 < Eg_2$). The lower band gap transitions are attributed to the O^{2-}-Co^{3-} (Eg_1) charge transfer and the higher band gap transitions are assigned to the O^{2-}-Co^{2-} (Eg_2) charge transfer processes. For the spinel-type cobalt oxide system, the presence of Co^{3-} centers creates sub-bands located inside the energy gap. Hence, Eg_2 is the actual band gap corresponding to inter-

band transition. For pure Co_3O_4, there were two optical transitions at 1.61 eV (Eg_1) and 1.86 eV (Eg_2).

It was found that the band gap energy value decreases for direct transitions when the Ag-content increases in the 2%, 6%, 13% and 24% Ag/Co_3O_4 system as indicated in Table 2.

Table 2. Band gap energy (direct transition) for 2%, 6%, 13% and 24% Ag/Co_3O_4 samples

Ag-content	Eg_1 (eV)	Eg_2 (eV)
0%	1,61	1,86
2%	1,61	2,00
6%	1,60	2,03
13%	1,52	1,60
24%	1,51	1,58

The decrease in Eg energy can be explained by the increase of silver content (Ag) in the Co_3O_4 that creates intra-band energy levels in the Co_3O_4 conduction band. These decreases indicate the enhancement in the electronic properties (high transport ability of electrons in the Co_3O_4 structure by the presence of silver).

3.4. BET studies

The specific area of the pure Co_3O_4 was calculated by BET to be 60 m^2/g but it decreases when the amount of silver increases. It decreases from 60 m^2/g for pure Co_3O_4 to 44 m^2/g and 37 m^2/g respectively for 13% and 24%Ag/Co_3O_4. This decrease could be due to partial blockage of the pores by the crystallites of the silver oxide.

3.5. Catalytic performance

The catalytic performances of the preferential oxidation of CO as a function of reaction temperatures for the studied catalysts prepared by the ammonia-evaporation - induced method are shown in Fig.4.

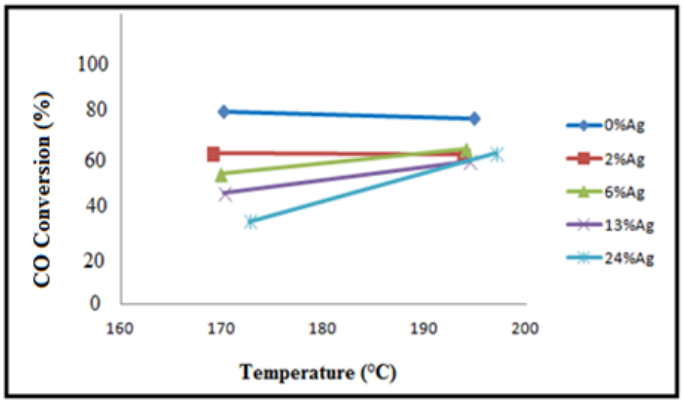

Fig.4. Conversion as a function of temperature for CO oxidation over 2%, 6%, 13% and 24% Ag/Co_3O_4 catalysts

Fig. 4 displays the CO oxidation activities of the samples as a function of the Ag loading for Ag/Co_3O_4 catalysts. It is clear that the activity of undoped Co_3O_4 catalysts is much

higher than that of silver doped Co_3O_4. Undoped cobalt oxide shows approximately 80% of CO conversion in the 170-195°C temperature range. This high conversion can be due to the mesoporous Co_3O_4 and a high BET surface area of 60 m^2/g. Fig. 4 shows that the CO conversion was effectively decreased by increasing the Ag content. This decrease can be caused by the variation in crystallite size as shown in Table 1, by the decreasing of the specific surface area from 60 m^2/g for undoped Co_3O_4 to 37 m^2/g for 24%Ag/Co_3O_4, and the decrease of the active sites on the cobalt oxide surface. The formation of carbon-coke on the cobalt oxide surface also has a great effect on the catalytic activity.

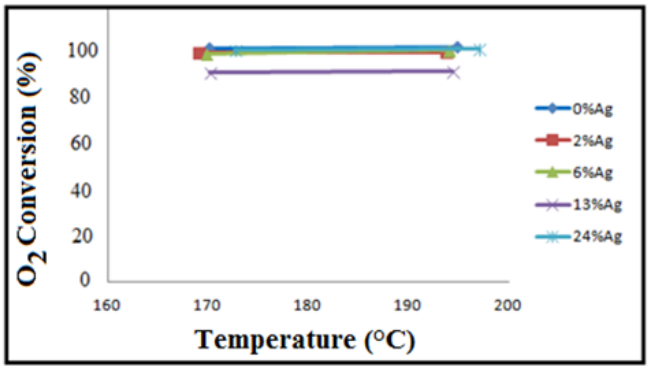

Fig. 5. Conversion of O_2 as a function of temperature over 2%, 6%, 13% and 24% Ag/Co_3O_4 catalysts

The conversion of O_2 is illustrated in Fig.5. O_2 conversion was around 100% in the 170-195°C temperature range regardless of the silver content.

4. Conclusion

In this work, a new and simple synthetic method for preparing metal wire meshes to support mesoporous (0%, 2%, 6%, 13% and 24%) Ag/Co_3O_4 was used. The structural, optical properties and catalytic activity of the resulting particles were investigated. Particle size was dependent of the silver content in cobalt oxide (Co_3O_4). When the amount of silver was equal to or larger than 13%, the nanorods broke, which could be due to the formation of Ag_2O and $AgCoO_2$. The band gap energy was found to decrease with the increase of silver content. Co_3O_4 nanorods supported over a metal wire mesh exhibit a high catalytic activity in the PROX reaction. The addition of silver content decreases the catalyst activity for the preferential oxidation of CO.

References

Afanasev, D.S., Yakovina, O.A., Kuznetsova, N.I., & Lisitsyn, A.S. (2012). High activity in CO oxidation of Ag nanoparticles supported on fumed silica. *Catalysis Communications*, *22*, 43-47.

Ahmed, S.R., Ogale, S., Papaefthymiou, G.C., Ramesh, R., & Kofinas, P. (2002). Magnetic properties of $CoFe_2O_4$ nanoparticles synthesized through a block copolymer nanoreactor route. *Applied Physics Letters*, 80, 1616-1618.

Alrehaily, L.M., Joseph, J.M., Biesinger, M.C., Guzonas, D.A., & Wren, J.C. (2013). Gamma-radiolysis-assisted cobalt oxide nanoparticle formation. *Physical Chemistry Chemical Physics*, 15, 1014-1024.

Avila, A.G., Barrera, E.C., Huerta, L.A., & Muhl, S. (2004). Cobalt oxide films for solar selective surfaces obtained by spray pyrolysis. *Solar Energy Materials and Solar Cells*, 82, 269-278.

Barkaoui, S., Dhaouadi, H., Kouassa, S., & Touati, F. (2015). Structural and optical proprieties of doped cobalt oxide: $Cu_xCo_{3-x}O_4$ (x = 0.0; 0.1; 0.2; 0.4; and 0.6). *Optik*, 126, 1047-1051.

Barkaoui, S., Haddaoui, M., Dhaouadi, H., Raouafi, N., & Touati, F. (2015). Hydrothermal synthesis of urchin-like Co_3O_4 nanostructures and their electrochemical sensing performance of H_2O_2. *Solid State Chemistry*, 228, 226-231.

Baydi, M.E., Poillerat, G., Rehspringer, J.L., Gautier, J.L., Koenig, J.F., & Chartier, P.J. (1994). A sol-gel route for the preparation of Co_3O_4 catalyst for oxygen electrocatalysis in alkaline medium. *Solid State Chemistry*, 109, 281-288.

Camargo, P.H.C., Satyanarayana, K.G., & Wypych, F. (2009). Nanocomposites: synthesis, structure, properties and new application opportunities. *Mat. Res*., 12, 1-39.

Chen, G.Si.X., Yu, J., Bai, H., & Zhang, X. (2015). Doping nano-Co_3O_4 surface with bigger nanosized Ag and its photocatalytic properties for visible light photodegradation of organic dyes. *Applied Surface Science*, 330, 191-199.

Cheng, Ch.S., Serizawa, M., Sakata, H., & Hirayama, T. (1998). Electrical conductivity of Co_3O_4 films prepared by chemical vapour deposition. *Material Chemistry and Physics*, 53, 225-230.

Craciun, R., Nentwick, B., Hadjiivanov, K., & Knozinger, H. (2003). Structure and redox properties of MnOx/Yttrium-stabilized zirconia (YSZ) catalyst and its used in CO and CH_4 oxidation. *Applied Catalysis*, A 243, 67-79.

Feng, K., Park, H.W., Wang, X., Lee, D.U., & Chen, Z. (2014). High Performance Porous Anode Based on Template-Free Synthesis of Co_3O_4 Nanowires for Lithium-Ion Batteries, Kun, *Electrochimica Acta*, 139, 145-151.

Gözüak, F., Köseoglu, Y., Baykal, A., & Kavas, H. (2009). Synthesis and characterization of $Co_xZn_{1-x}Fe_2O_4$ magnetic nanoparticles via a PEG-assisted route. *J. Magn. Magn. Mater*., 321, 2170-2177.

Guldur, C., Balikci, F. (2002). Selective carbon monoxide oxidation over Ag-based composite oxides. *Int. J. Hydrogen Energy*, 27, 219-224.

Gupta, R.K., Sinha, A.K., Raja Sekhar, B.N., Srivastava, A.K., Singh, G., & Deb, S.K. (2011). Synthesis and characterization of various phases of cobalt oxide nanoparticles using inorganic precursor. *Appl. Phys. A*, 103, 13-19.

Hosny, N.M. (2014). Single crystalline Co_3O_4: Synthesis and optical properties, *Mater. Chem. Phys*., 144, 247-251.

Hu, L., Sun, K., Peng, Q., Xu, B., & Li, Y. (2010). Surface active sites on Co_3O_4 nanobelt and nanocube model catalysts for CO oxidation. *Nano Res*., 3, 363-368.

Huang, R., Shen, Y., Zhao, L., & Yan, M. (2012). Effect of hydrothermal temperature on structure and photochromic properties of WO_3 powder. *Adv. Powder Technol*., 23, 211-214.

Imamura, S., Sawada, H., Uemura, H., & Ishida, S. (1988). Oxidation of carbon monoxide catalyzed by manganese-silver composite oxides. *J. Catal.*, 109, 198-205.

Ishaque, M., Islam, M.U., Khan, M.A., Rahman, I.Z., Genson, A., & Hampshire, S. (2010). Structural, electrical and dielectric properties of yttrium substituted nickel ferrites. *Phys. B Condens. Matter.*, 405, 1532-1540.

Keshavaraja, A., She, X., & Flytzani-Stephanopoulos, M. (2000). Selective catalytic reduction of NO with methane over Ag-alumina catalysts. *Appl. Catal. B*, 27, L1-L9.

Li, Y., Tan, B., & Wu, Y. (2008). Mesoporous Co_3O_4 nanowire arrays for lithium ion batteries with high capacity and rate capability. *Nano Letters*, 8, 265-270.

Makhlouf, S.A., Bakr, Z.H., Aly, K.I., & Moustafa, M.S. (2013). Structural, electrical and optical properties of Co_3O_4 nanoparticles, *Superlattices Microstruct.*, 64, 107-117.

Moro, F., Tang, S.V.Y., Tuna, F., Lester, E. (2013). Magnetic properties of cobalt oxide nanoparticles synthesised by a continuous hydrothermal method. *Journal of Magnetism and Magnetic Materials*, 348, 1-7.

Pudukudy, M., Yaakob, Z. (2014). Sol-gel synthesis, characterisation, and photocatalytic activity of porous spinel Co_3O_4 nanosheets. *Chem. Pap.*, 68, 1087-1096.

Rahman, M.M., Wang, J.Z., Deng, X.L., Li, Y., & Liu, H.K. (2009). Hydrothermal synthesis of nanostructured Co_3O_4 materials under pulsed magnetic field and with an aging technique, and their electrochemical performance as anode for lithium-ion battery. *Electrochim. Acta*, 55, 504-510.

Sandoval, A., Aguilar, A., Louis, C., Traverse, A., Zanella, R. (2011). Bimetallic Au-Ag/TiO_2 catalyst prepared by deposition-precipitation: High activity and stability in CO oxidation, *J. Catal.*, 281, 40-49.

Sarfraz, A.K., Hasanain, S.K. (2014). Size Dependence of magnetic and optical Properties of Co_3O_4 Nanoparticles, *Acta Phys. Pol. A*, 125, 139-144.

Wang, G., Shen, X., Horvat, J., Wang, B., Liu, H., Wexler, D. (2009). Hydrothermal synthesis and optical, magnetic, and supercapacitance properties of nanoporous cobalt oxide nanorods. *J. Phys. Chem. C*, 113, 4357-4361.

Wang, X., Zheng, R., Liu, Z., Ho, H., Xu, J., Ringer, S., P. (2008). Structural, optical and magnetic properties of Co-doped ZnO nanorods with hidden secondary phases. *Nanotechnology*, 19, 455702.

Wu, L., Wang, Z-X., Li, X.-H., Li, L., Guo, H.-J., Zheng, J.-Ch., Wang, X.-J. (2010). Electrochemical performance of Ti^{4+}-doped $LiFePO_4$ synthesized by co-precipitation and post-sintering method. *Trans. Nonferrous Met. Soc. China*, 20, 814-818.

Zamiri, R., Singh, B.K., Dutta, D., Reblo, A.J., Ferreira, M.F. (2014). Electrical properties of Ag-doped ZnO nano-plates synthesized via wet chemical precipitation method. *Ceram. Int.*, 40, 4471-4477.

Zhang, X., Qu, Zh., Li, X., Wen, M., Quan, X., Ma, D., Wu, J. (2010). Studies of silver species for low-temperature CO oxidation on Ag/SiO_2 catalysts. *Sep. Purif. Technol.*, 72, 395-400.

Zhao, Z., Lin, X., Jin, R., Wang, G., Muhammad, T. (2012). MO_x (M = Mn, Fe, Ni or Cr) improved supported Co_3O_4 catalysts on ceria-zirconia nanoparticulate for CO preferential oxidation in H_2-rich gases. *Applied Catalysis B*: *Environmental*, 115-116, 53-62.

Zou, D., Xu, C., Luo, H., Wang, L., Ying, T. (2008). Synthesis of Co_3O_4 nanoparticles via an ionic liquid-assisted methodology at room temperature. *Mater. Lett.*, 62, 1976-1978.